EUROPEAN SOUTHERN OBSERVATORY

Organisation Européenne pour des Recherches Astronomiques dans l'Hémisphère Austral

Europäische Organisation für astronomische Forschung in der südlichen Hemisphäre

LA SILLA OBSERVATORY
NEW TECHNOLOGY TELESCOPE

Study on SOFI

—

**Distorsion on the Small Field SOFI
Report**

Doc. No. LSO-TRE-ESO-40200-1062

Issue 1.01

Date 23/09/03

Prepared for Review - INTERNAL USE ONLY

Prepared . . . . C. Ducourant & M. Rapaport   23/09/03 . . . .
| | Name | Date | Signature |

Reviewed . . . . M. Billères   23/09/03 . . . .
| | Name | Date | Signature |

Approved . . . . . . O. Hainaut . . . .
| | Name | Date | Signature |

Released . . . . xxx . . . .
| | Name | Date | Signature |

This page was intentionally left blank

Change Record

Issue/Rev.	Date	Section/Parag. affected	Reason/Initiation/Documents/Remarks
C. Ducourant M. Billères	September 2003 23/09/03	....	Creation Formatting

This page was intentionally left blank

Contents

This page was intentionally left blank

Abstract

The IR imaging with the NTT small field SOFI camera is known to produce significative distorsions of the images. No astrometric quantification of these distorsions nor corrections have been produced yet. We have studdied these distorsions and we show that they reach 0.352 pixel = 50 mas and we propose a table of correction to apply to any measurement.

1   Introduction

We began in April 2000 at the NTT a program of infrared high accuracy astrometry. Our program was designed for the SOFI infrared camera operated in its small field configuration. It appeared that in this mode there exist large optical distorsions in the field whose impact on astrometry are not known but strongly suspected. The astrometric objective of our program was very ambitious and could not suffer such effects. Therefore we decided to start a parallel program to map these distorsions, evaluate their impact on the astrometry and propose a table of correction to remove them from the observations.

Our idea was to perform numerous overlapping observations of a dense region of the sky (Omega Centauri cluster) with a very large area of overlap. Then each star of the field would be observed at several places of the detector. Assuming that the distorsions do not affect more than 1/5 of the field (which is in agreement with the apparent distorsions of star images, as observed by eye) then a global resolution of the system with a 3σ elimination will lead to "mean" positions for the stars that should not be significantly affected by the astrometric systematic effects. Then a comparison of the individual positions and this mean position would lead us to map the distorsion as function of the position of the image on the detector.

2   The data

We have used in this work 25 images of the Omega centauri globular cluster ($\alpha_{2000} = 13^h 26^m 45.89^s$, $\delta_{2000} = 47^o 28' 36.7''$) taken at the NTT in july 2000 to study the field distorsions of the SOFI small field imaging (1024 x 1024 pixels, 1 pixel = 0.144'', Fov = 2.4 ' x 2.4'). The 25 images are offsetted one from the other of about 140 pixels (overlapping pattern given in Fig. 1). Therefore each star is observed at several places of the detector as shown in fig 2. The mean seeing of these images was 6 pix = 0.9 arsec. We give in Fig. 3 a 5 arcmin x 5 arcmin IR image of Omega centauri cluster (Digital sky survey, second epoch, IR) corresponding to the observed zone. We give in Fig. 4 the NTT Small Field SOFI image of the first field.

3   Cross-identification of the images

Individual images have been reduced using the ECLIPSE package and measured using the DAOPHOT package fitting a PSF (Moffat function). For the reduction process we have first cross-identified each image with each of the others images. This cross identification is based on two steps: first the program test each possible triangle in an image and looks for it in the other image with a tolerance level on the three lengths between 0.1 to 1 pixels depending on the image quality. When a possible solution is found then the program applies a standard 2x3 constant reduction model between the two sets of measurements and looks for all possible coincidences. If the number of coincidences is large enough (larger than 15) then the solution is adopted; in the opposite case another triangle is tested. We give in Fig. 5 the histogram of the number of coincidences between pairs of images. One can see that there are about 50 stars in common in each pair of images.

Then, the files containing the cross-identifications of pairs of images have been collected, and we produced a catalogue of the 379 stars presents in the 3.84'x3.84' field. This catalogue contains for each star all its measured coordinates on the images where it has been detected, summing up 2759 (x,y) measurements. We give in Fig. 6 the distribution of errors on internal magnitudes given by DAOPHOT as function of internal magnitudes of these measurements.

From these measurements we only kept the 1978 measurements with an error on internal magnitude lower than 0.08.
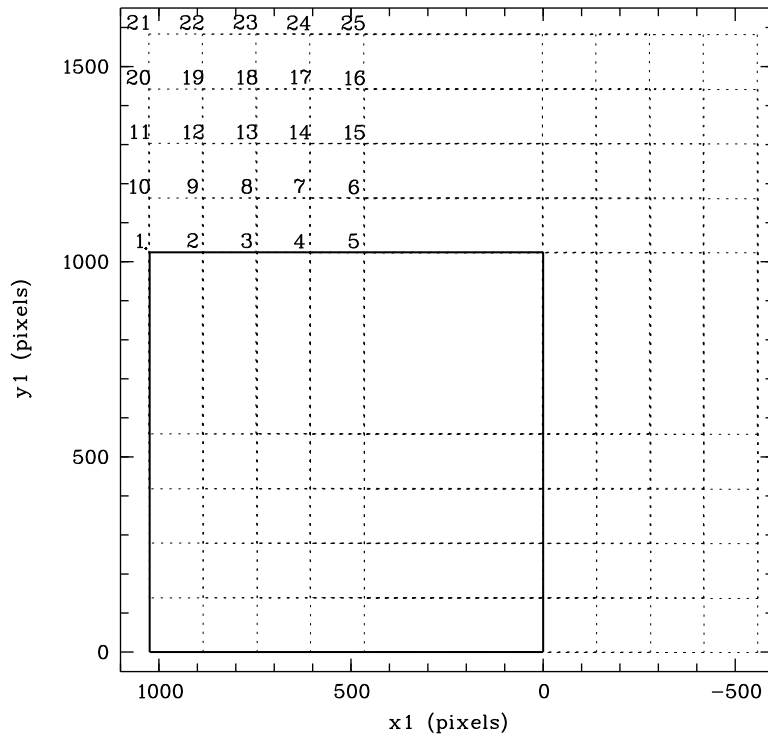
Figure 1: The 25 overlapping images. plain line correspond to the first image. 1 pixel = 0.144 arcsec. Covered field = 1600 x 1600 pix = 3.84' x 3.84', the numbers of the fields are placed at the upper left limit of each field. North is up and increasing right ascensions left.
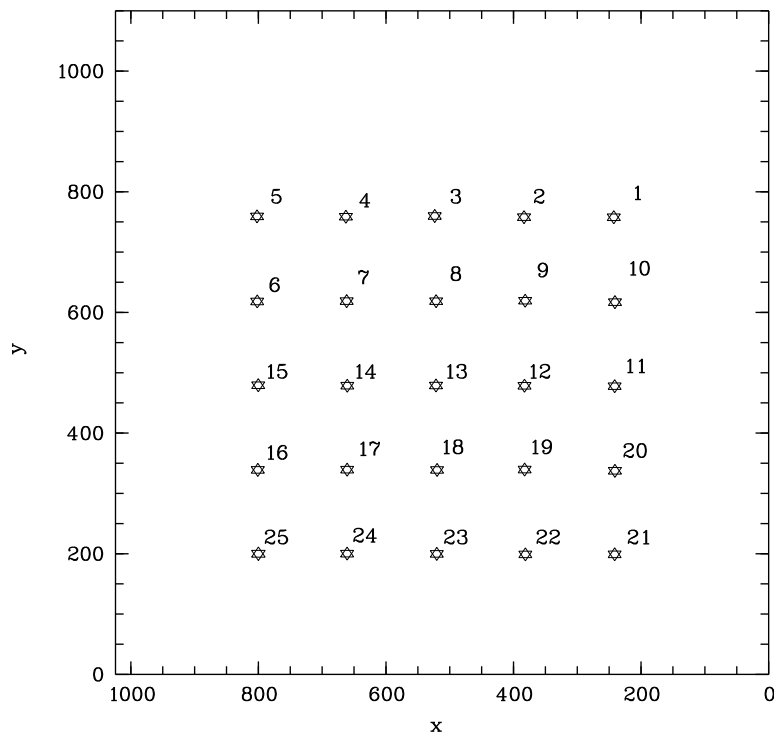

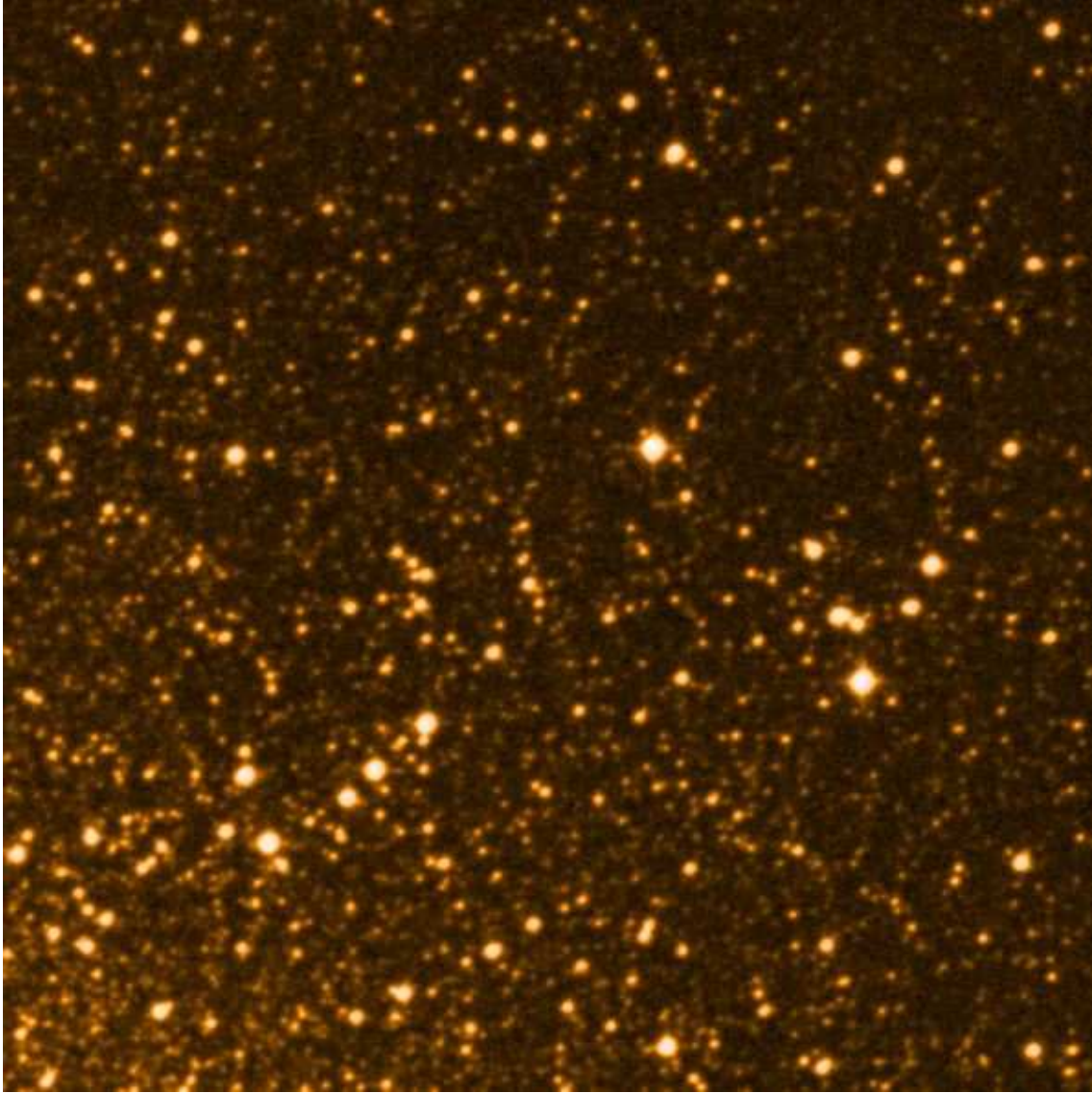Figure 2: Each star will be observed at different places of the matrix as illustrated here.

Figure 3: 5' x 5' IR image of Omega centauri cluster from DSS2. North is up and increasing right ascensions left.
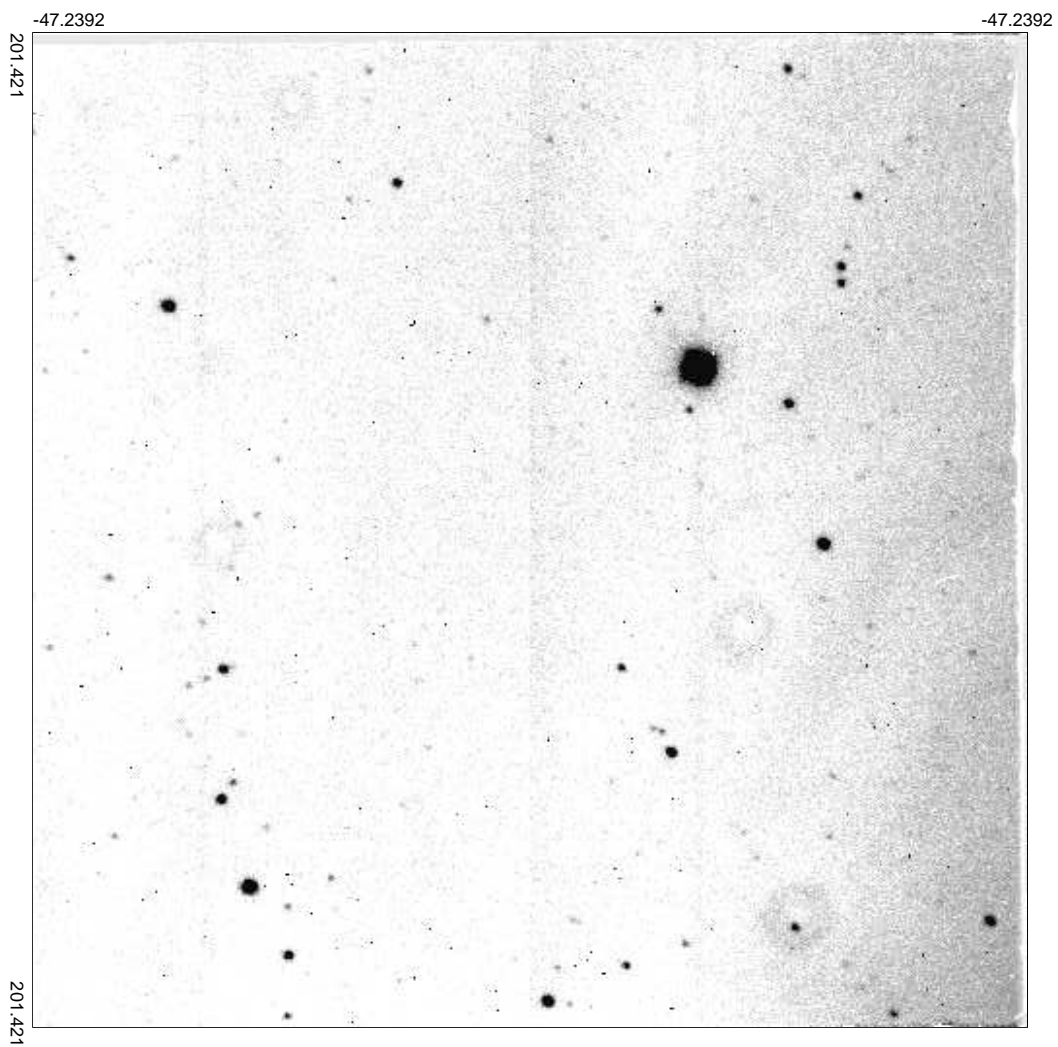
Figure 4: First image (J filter) (2.46' x 2.46') of the 25 exposures. North is up and increasing right ascensions left.
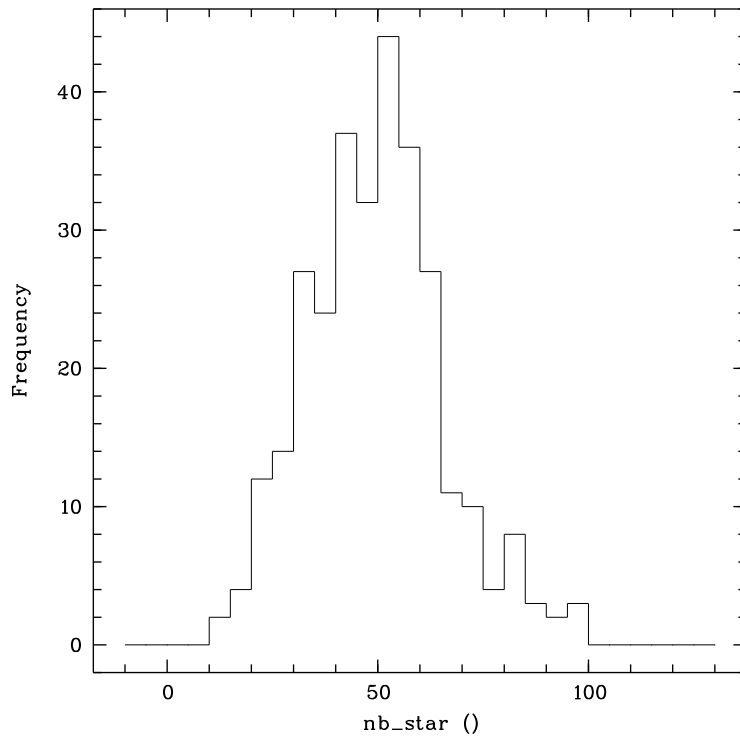
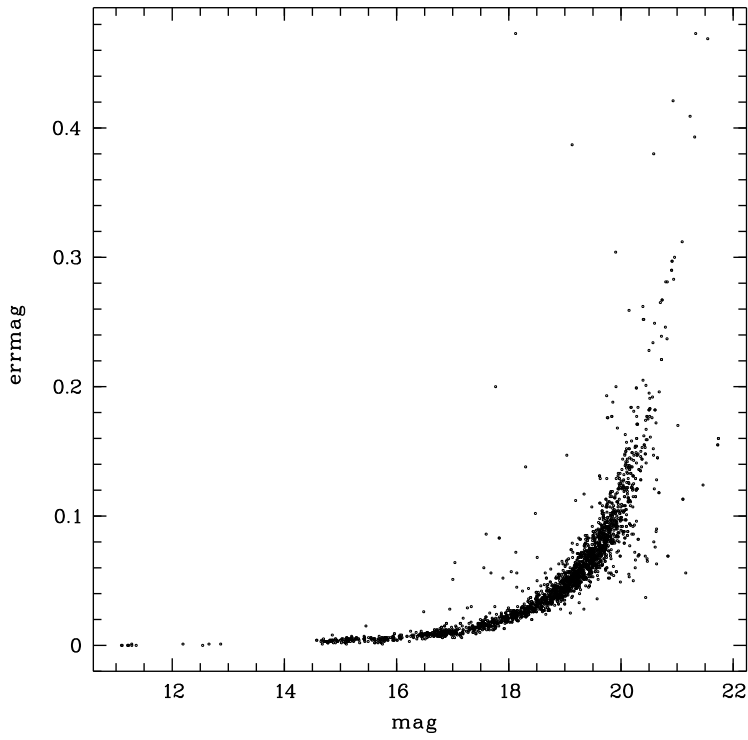Figure 5: Histogram of the number of coincidences between pairs of images.

Figure 6: Distribution of errors on internal magnitudes given by DAOPHOT as function of internal magnitudes for the 2549 measurements.
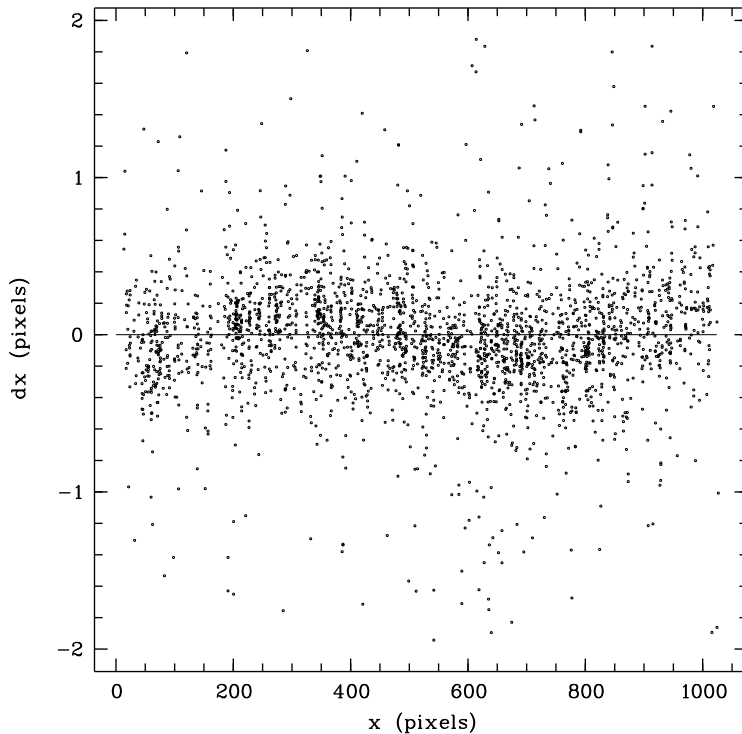
Figure 7: Distance between individual observations and mean position of each star in x coordinate as function of its x measurement.

4   Global reduction

We have performed an iterative global solution of the whole system, solving the equations:

$$X + \Delta X = a_i x + b_i y + c_i$$
$$Y + \Delta Y = a_i x + b_i y + c_i$$

Where (X,Y) are estimates of the position of the stars in the reference system of the solution, typically (X,Y) are the means of the individual measurements transported in the reference system of the solution. Where (x,y) are the individual measurements of the stars on each frame. Where a_i, b_i, c_i are the instrumental constants relative to the ith frame which link the measurements of the stars on the ith frame to the coordinate of the star in the reference system of the solution. On the first iteration the instrumental constants are determined then the offsets (ΔX, ΔY) to the final position of the stars are determined and the process iterates until the modification of the rms of the global adjustment is less than 0.01 pixel (1.5 mas). An elimination of abnormal observations at a 3σ level is performed at each iteration. The system converges rapidly (3 or 4 iterations).

This global reduction lead us to the estimation of the relative positions of the 379 stars with a mean precision of 34 mas (0.223 pixels).

5   Mapping of the distortions

We calculated the distance between individual positions of the stars on the 25 images (transported to the reference solution frame) to the calculated position of the stars by the global solution. We give in Fig. 7,8,9,10 these distances in x and y coordinates as function of x and of y measurements.

One notice easily on these diagrams that there exist distortions which depend on the position in the field. We give in Fig. 11 the mean of the distances between the individual measurements and the final global position of the stars in squares of 120 pixels .
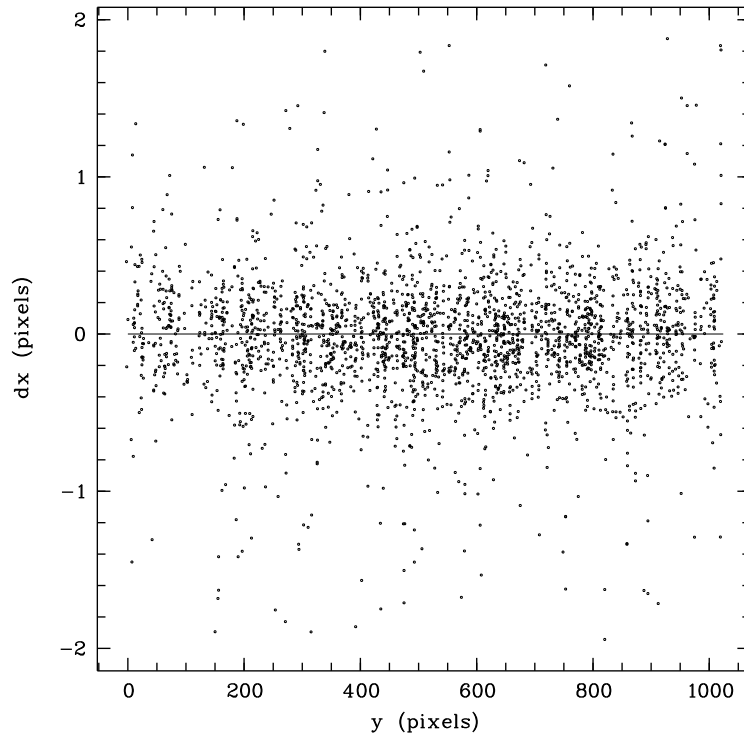
Figure 8: Distance between individual observations and mean position of each star in x coordinate as function of its y measurement.
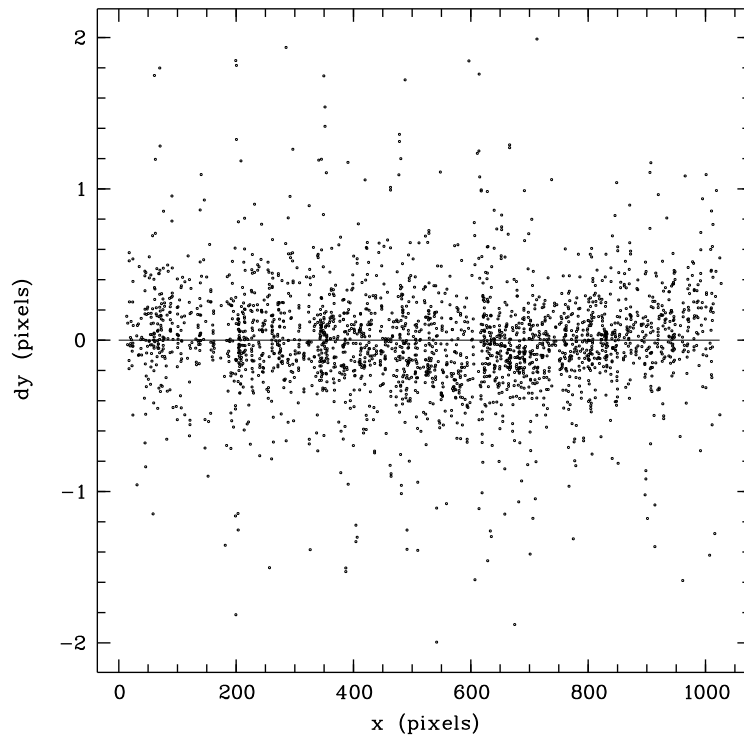

Figure 9: Distance between individual observations and mean position of each star in y coordinate as function of its x measurement.
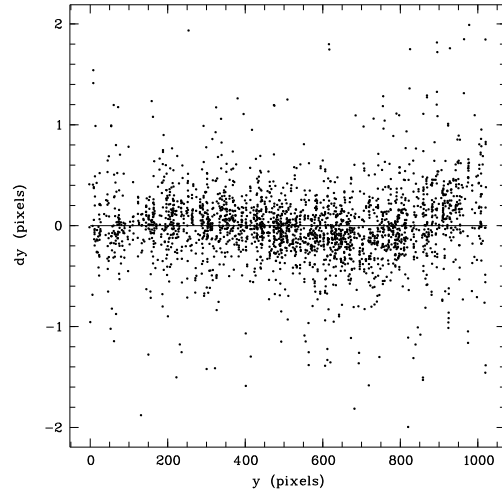
Figure 10: Distance between individual observations and mean position of each star in y coordinate as function of its y measurement.
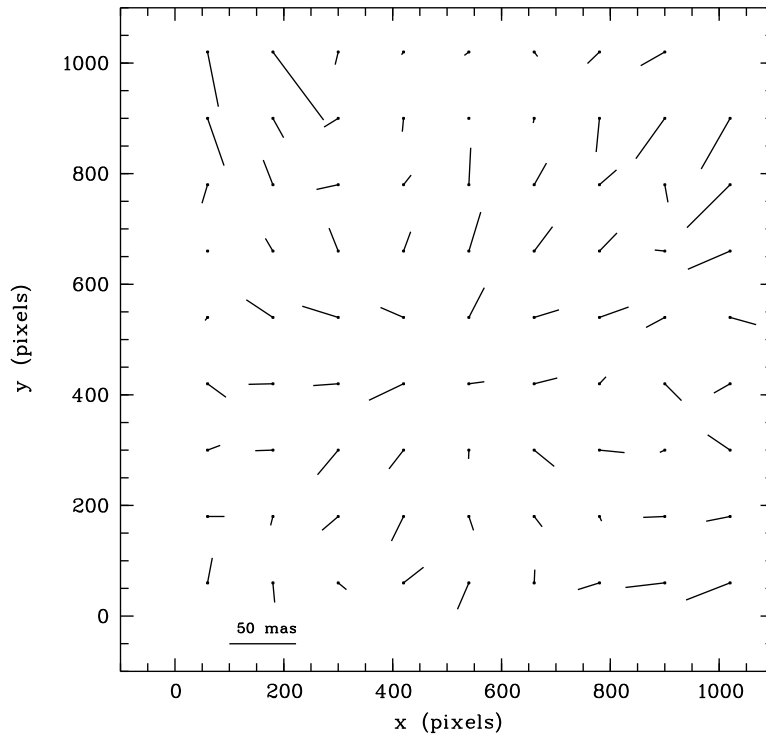

Figure 11: Pattern of distortions in the NTT SOFI small field expressed as function of (x,y) measurements. Distortions are calculated in 120 pixel squares.
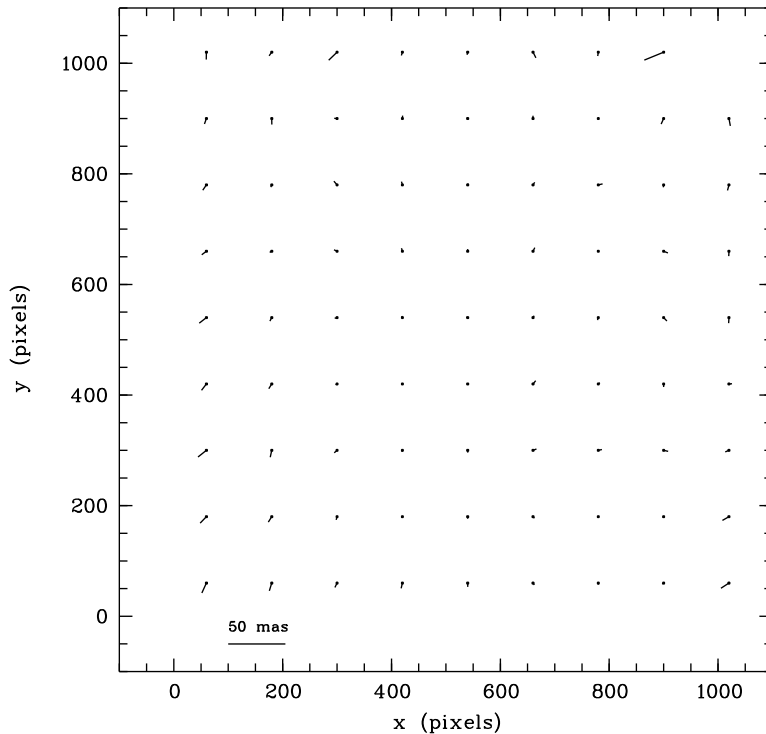
Figure 12: Pattern of distortions in the NTT SOFI small field expressed as function of (x,y) measurements after correction of the distorsions.

We give in table 1 the mean corrections derived from this work in the 120 pixel squares . One can see that these systematic effects that affect the measurements can reach 0.352 pixels (50 mas).

To correct measurements performed on images aligned on the sky one should : 1)check that increasing x coordinate correspond to decreasing right ascension, that increasing y coordinate follows increasing declination. 2) apply the correction :

$$x = x - dx$$
$$y = y - dy$$

Where (x,y) are the measurements in pixels.
Where dx,dy,weight are given by columns 1,2,5 of table 1 for boxes centered on (x,y) (columns 3 and 4) and with a width of 120 pixels.

6   Correction of the measurements and final global solution

We have corrected the individual measurements of the 379 stars present in the 25 images using this table of correction and calculated a global adjustment of the system. Then we have re-calculated a table of pattern, re-applied it, and iterated 3 times. The rms of the final global solution is now 27 mas which is to be compared with the value obtained with uncorrected measurements (rms = 34 mas). Then we re-calculated the remaining pattern in 120 pixel squares to check the efficiency of the correction. We give in Fig. 12 the remaining pattern after correction of the individual measurements.

After correction of the measurements it is clear that the major systematic effects are removed from the data except on the very border of the matrix and never exceed 11 mas .

Table 1: The pattern coefficients dx and dy.

dx [pix]	dy [pix]	x [pix]	y [pix]
-0.054	-0.086	60.	60.
-0.057	0.096	60.	180.
0.082	0.080	60.	300.
-0.056	0.139	60.	420.
0.130	0.067	60.	540.
0.038	0.049	60.	660.
0.045	0.238	60.	780.
-0.095	0.412	60.	900.
-0.096	0.530	60.	1020.
0.031	0.230	180.	60.
0.083	0.135	180.	180.
0.120	0.083	180.	300.
0.189	0.073	180.	420.
0.182	-0.063	180.	540.
0.089	-0.084	180.	660.
0.087	-0.096	180.	780.
-0.106	0.224	180.	900.
-0.291	0.464	180.	1020.
-0.009	0.104	300.	60.
0.103	0.143	300.	180.
0.203	0.197	300.	300.
0.179	0.024	300.	420.
0.261	-0.094	300.	540.
0.158	-0.187	300.	660.
0.130	0.017	300.	780.
0.131	0.025	300.	900.
0.067	0.150	300.	1020.
-0.135	-0.030	420.	60.
0.104	0.138	420.	180.
0.121	0.076	420.	300.
0.272	0.114	420.	420.
0.169	-0.073	420.	540.
-0.036	-0.189	420.	660.
-0.030	-0.130	420.	780.
0.055	0.046	420.	900.
0.028	0.050	420.	1020.
0.083	0.228	540.	60.
-0.018	0.129	540.	180.
-0.010	0.083	540.	300.
-0.105	-0.026	540.	420.
-0.101	-0.237	540.	540.
-0.045	-0.273	540.	660.
-0.023	-0.252	540.	780.
-0.002	-0.026	540.	900.
0.043	0.021	540.	1020.
-0.021	-0.089	660.	60.

Table 2: second part ... The pattern coefficients.

dx [pix]	dy [pix]	x [pix]	y [pix]
-0.118	0.114	660.	180.
-0.180	0.124	660.	300.
-0.181	-0.076	660.	420.
-0.179	-0.096	660.	540.
-0.162	-0.195	660.	660.
-0.115	-0.188	660.	780.
0.002	0.027	660.	900.
-0.064	0.096	660.	1020.
0.112	0.074	780.	60.
-0.013	0.048	780.	180.
-0.148	-0.002	780.	300.
-0.098	-0.072	780.	420.
-0.204	-0.084	780.	540.
-0.152	-0.085	780.	660.
-0.128	-0.102	780.	780.
0.048	0.226	780.	900.
0.104	0.155	780.	1020.
0.247	0.075	900.	60.
0.157	0.022	900.	180.
0.034	0.040	900.	300.
-0.121	0.127	900.	420.
0.086	0.082	900.	540.
0.058	-0.001	900.	660.
-0.031	0.148	900.	780.
0.285	0.383	900.	900.
0.246	0.298	900.	1020.
0.459	0.193	1020.	60.
0.370	0.078	1020.	180.
0.196	-0.071	1020.	300.
0.170	0.106	1020.	420.
-0.167	0.171	1020.	540.
0.257	0.212	1020.	660.
0.326	0.436	1020.	780.
0.250	0.540	1020.	900.

7   Conclusion

In this work we have studied the optical distortion of the NTT SOFI small field configuration. We showed that these distortions affect essentially one border of the camera. From these, result displacements of the photocenter of the images that reach 50 mas. We propose a table of correction of measurements to remove the effects from the data.

__oOo__